

The GW plus cumulant method and plasmonic polarons: application to the homogeneous electron gas

Fabio Caruso and Feliciano Giustino

Department of Materials, University of Oxford, Parks Road, Oxford OX1 3PH, United Kingdom

(Dated: August 28, 2018)

We study the spectral function of the homogeneous electron gas using many-body perturbation theory and the cumulant expansion. We compute the angle-resolved spectral function based on the *GW* approximation and the ‘*GW* plus cumulant’ approach. In agreement with previous studies, the *GW* spectral function exhibits a spurious plasmaron peak at energies $1.5\omega_{\text{pl}}$ below the quasiparticle peak, ω_{pl} being the plasma energy. The *GW* plus cumulant approach, on the other hand, reduces significantly the intensity of the plasmon-induced spectral features and renormalizes their energy relative to the quasiparticle energy to ω_{pl} . Consistently with previous work on semiconductors, our results show that the HEG is characterized by the emergence of plasmonic polaron bands, that is, broadened replica of the quasiparticle bands, red-shifted by the plasmon energy.

I. INTRODUCTION

The homogeneous electron gas (HEG) denotes a model system of electrons interacting with a compensating homogeneous positively-charged background.¹ The model, because of its simplicity, lends itself to analytical treatment and has therefore provided the ideal test-case for the early development of many-body perturbation theory.² Despite the simplicity of the model, the HEG provides valuable insight into the physical properties of real systems, such as crystalline solids, as it exhibits prototypical features induced by electronic correlation. For example, the dielectric function of the HEG exhibits signatures of collective charge-density fluctuations, that is plasmons,³ and the study of these features has led to the interpretation of the satellite structures in the early electron-energy loss spectroscopy (EELS) measurements of simple metals.⁴ Overall, the study of plasmons has played an important role in the early development of many-body perturbation theory. The random-phase approximation (RPA), for example, was originally introduced by Pines and Bohm⁵ as a simplification of the equation of motion for the density fluctuation in the HEG.

In the context of spectroscopy the study of plasmon-induced signatures in the spectral function of the HEG has contributed (i) to elucidate the fundamental processes that underpin the emergence of satellites in photoelectron spectra^{6,7}, and (ii) to derive new theoretical tools for their description.⁸ Calculations based on the *GW* approximation^{9,10} do not generally provide an accurate description of plasmon-induced spectral features. Both in the HEG^{11,12} and in real solids,^{13,14} (for example silicon) the *GW* approximation introduces a spurious ‘plasmaron’ peak in the spectral function, that is a sharp quasiparticle-like feature that arises from an additional solution of the Dyson equation. At first, the plasmaron was attributed to a novel type of quasiparticle excitation resulting from the strong coupling between electrons and plasmons.^{11,12} Later studies revealed that the plasmaron solution is an artifact of the *GW* approach, and

disappears when a higher level of theory is employed, such as the cumulant expansion.⁸ The cumulant expansion approach is the state-of-the-art technique for the description of satellites in photoemission and it accounts for the interaction between electrons and plasmons employing an independent boson model.¹⁵ This model is exactly solvable for a single core electron interacting with a plasmon bath, and it provides an explicit expression for the spectral function.^{8,16} Beside the first cumulant studies of the HEG, the cumulant expansion has been extended^{17,18} and applied to describe the spectral signatures of plasmons in the valence photoelectron spectra of metals,^{17,19,20} semiconductors,^{14,21–24} and models systems.^{25,26} The cumulant approach proved useful also in the computation of total energies²⁷ and ultrafast quasiparticle dynamics.^{28–30}

In this work, we present a study of the spectral function and the signatures of electron-plasmon interaction in the HEG based on the *GW* approximation and the *GW* plus cumulant (*GW*+*C*) approach. We first review the characterization of electronic excitations through the computation of the RPA dielectric function. We thus compute the angle-resolved spectral function of the HEG in the *GW* approximation to illustrate the emergence of the spurious plasmaron peak. Finally, we present calculations of HEG spectral function based on the *GW*+*C* approach. Our calculations show that the *GW*+*C* approach renormalizes the energy of the plasmon-induced spectral features to $\sim \omega_{\text{pl}}$ below the quasiparticle energy, consistently with previous work. Additionally, the analysis of the energy-momentum dispersion relations reveals the emergence of a plasmonic polaron band, which manifests itself as a broadened replica of the quasiparticle band, red-shifted by the plasmon energy. This result further validates the concept of plasmonic polaron band, originally proposed for simple semiconductors^{23,24,31} and confirmed through angle-resolved photoemission measurements in silicon.³¹

The manuscript is organized as follows. In Sec. II, we present calculations of the loss function of the HEG in the RPA. The *GW* approximation and its application to the spectral properties of the HEG are discussed in Sec. III,

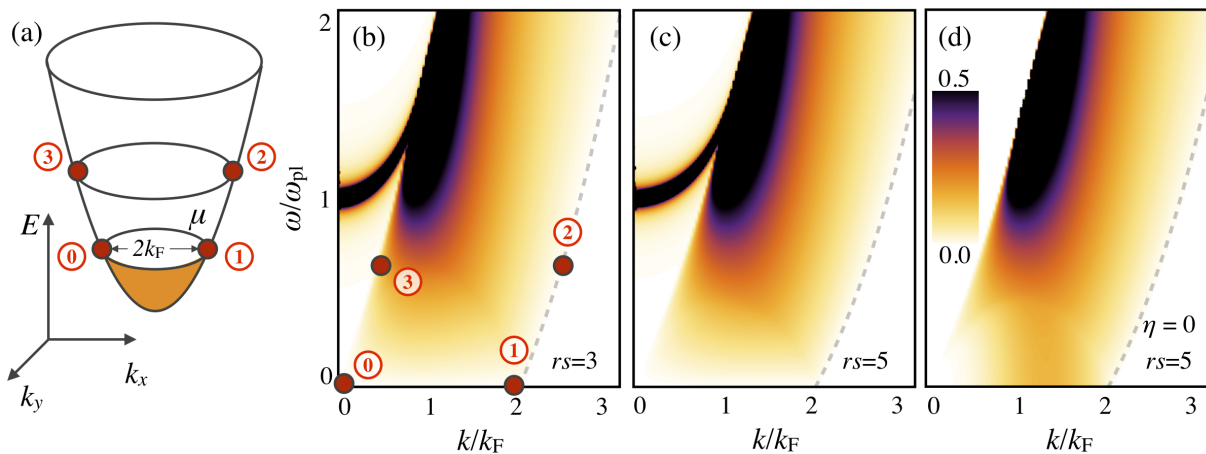


Figure 1. Schematic representation of the parabolic band dispersion of the HEG. The red circles ('1', '2', and '3') indicate some representative final states for electron-hole excitations starting from the initial state '0' at the Fermi energy μ . (b)-(c) RPA loss function of the HEG evaluated in the GW approximation at the densities $r_s = 3$ (b) and $r_s = 5$ (c). Here we considered frequencies with a small imaginary component ($\eta \sim 0.004 \times \mu$) to clearly visualize the plasmon peak. The case $\eta = 0$ is shown in (d) for $r_s = 5$. Energy and momentum are expressed in units of the plasmon energy ω_{pl} and Fermi momentum k_F , respectively. The circles (0, 1, 2, and 3) in panel (b) are placed at points where the intensity of the loss function arises from the transitions illustrated in panel (a).

whereas in Sec. IV we present calculations of the HEG spectral function based on the $GW+C$ approach. Finally, our conclusions are presented in Sec. V.

II. SIGNATURES OF PLASMONS IN THE DIELECTRIC FUNCTION

Electronic excitations of the HEG can be characterized through the computation of the loss function:³²

$$\mathcal{L}(\mathbf{q}, \omega) = \text{Im} \epsilon^{-1}(\mathbf{q}, \omega), \quad (1)$$

where ϵ is the dielectric function. Since the dielectric function vanishes at the frequencies resonant with the excitations of plasmons,³³ the loss function exhibits pronounced singularities at the plasmon energies $\omega_{\text{pl}}(\mathbf{q})$. The condition $\epsilon[\mathbf{q}, \omega_{\text{pl}}(\mathbf{q})] = 0$,³⁴ which defines the plasmon energy, provides a rationale to distinguish between spectral signatures of plasmon and electron-hole pairs in the loss function. In particular, plasmons are expected to induce Dirac-delta-like features in Eq. (1), well separated from the continuum of electron-hole pair excitations.

In a Green's function formalism, the dielectric function may be expressed as:

$$\epsilon(\mathbf{q}, \omega) = 1 - v(\mathbf{q})\chi_0(\mathbf{q}, \omega), \quad (2)$$

where we introduced the irreducible polarizability χ_0 and the bare Coulomb interaction $v(\mathbf{q}) = 4\pi/|\mathbf{q}|^2$. Here and in the following we adopted Hartree atomic units, unless otherwise stated. In the RPA, whereby electron-hole interactions are neglected, χ_0 may be expressed explicitly

as:⁷

$$\chi_0(\mathbf{q}, \omega) = -i \int \frac{d\mathbf{k} d\omega'}{(2\pi)^4} G_0(\mathbf{q} + \mathbf{k}, \omega + \omega') G_0(\mathbf{k}, \omega'). \quad (3)$$

We introduced here the non-interacting Green's function, defined by:

$$G_0(\mathbf{k}, \omega) = \frac{1}{\omega + \mu - \epsilon_{\mathbf{k}} + i\text{sign}(\mu - \epsilon_{\mathbf{k}})}, \quad (4)$$

where μ is the Fermi energy, $\epsilon_{\mathbf{k}} = k^2/2$, and η a positive infinitesimal. The convolution in Eq. (3) may be carried out analytically,³³ yielding an explicit expression for the dielectric function of the HEG:^{9,15}

$$\epsilon(q, \omega) = 1 + \frac{\alpha r_s}{8\pi q^3} [H(q + u/q) - H(q - u/q)], \quad (5)$$

where $H(q) = 2q + (1 - q^2)\ln[(q + 1)/(q - 1)]$, $\alpha = (4/9\pi)^{1/3}$. Here we followed the notation of Ref. 9 where q denotes momenta in units of $2k_F$ and u are energies in units of 4μ . r_s denotes the Wigner-Seitz radius. The calculation of the loss function is reduced to the evaluation of the Eq. (5) for several frequencies and momenta.

In Fig. 1 we report the loss function of the HEG for $r_s = 3$ (b) and $r_s = 5$ (c). A detailed discussion of the loss function may be found in many textbooks.^{15,35} Briefly, the broad band of width $2k_F$ is the continuum of electron-hole excitation. To exemplify the origin of these features we report in Fig. 1 (a) a schematic representation of the free electron energy band of the HEG. The labels '1', '2', and '3' denote possible final states for the excitation of an electron at the Fermi energy (red dot labelled '0'). The transition to 1 involves a

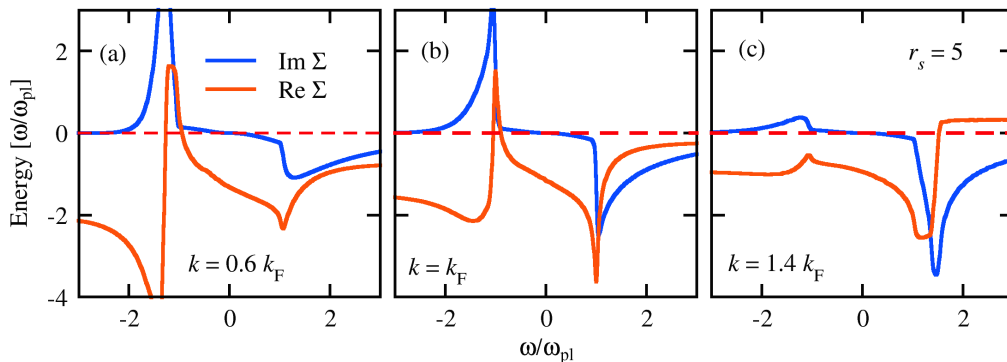


Figure 2. *GW* self-energy of the HEG for $r_s = 5$ at $k = 0.6k_F$ (a), $k = k_F$ (b), and $k = 1.4k_F$ (c). The energy is in units of the plasmon energy, $\omega_{pl} = 4.2$ eV.

very small change of energy and a momentum transfer of $\sim 2k_F$. The contribution of these transition to the loss function is infinitesimal due to the small phase space available for the transitions. By considering finite energy changes, electron-hole excitations must necessarily involve a change of momentum. The maximum (minimum) momentum transfer would correspond to transition of the type 2 (3). The corresponding signatures of these transitions in the loss function are indicated by 1, 2, and 3 in Fig. 1 (b). According to the previous discussion, the high-intensity feature at small momentum transfer may not be attributed to electron-hole excitations. This feature is the plasmon peak and stems from the zeros of dielectric function. In particular, for $k = 0$, the plasmon peak occurs exactly at the plasma energy ω_{pl} . At energies and momenta at which the plasmons and the electron-hole excitations coexist, the plasmon peak is broadened out and its spectral features are not distinguishable from the electron-hole continuum.

To visualize the plasmon peak of the loss function we considered frequencies with a small imaginary part ($\eta = 0.004 \times \mu$). If purely real frequencies were considered, the plasmon peak would not be visible in the loss function owing to the finite momentum resolution in the figure [Fig. 1 (d), for $r_s = 5$]. We now move on to discuss the spectral function of the HEG in the *GW* approximation and the spectral signatures of plasmons.

III. *GW* SELF-ENERGY AND SPECTRAL FUNCTION OF THE HEG

In the *GW* approximation, the electron self-energy for the HEG takes the form:

$$\Sigma(\mathbf{k}, \omega) = \frac{i}{2\pi} \int d\omega' d\mathbf{q} G(\mathbf{k} + \mathbf{q}, \omega + \omega') W(\mathbf{q}, \omega). \quad (6)$$

The screened Coulomb interaction W can be expressed as:

$$W(\mathbf{q}, \omega) = \frac{v(\mathbf{q})}{\epsilon(\mathbf{q}, \omega)}. \quad (7)$$

In principle, the evaluation of the self-energy in Eq. (6) should employ a Green's function obtained self-consistently from the solution of the Dyson's equation:

$$[G(\mathbf{k}, \omega)]^{-1} = [G_0(\mathbf{k}, \omega)]^{-1} - \Sigma(\mathbf{k}, \omega). \quad (8)$$

Self-consistent *GW* denotes the procedure in which Eqs. (2), (3), (6), (7), and (8) are iterated until convergence is reached. For atoms and molecules it is well established that self-consistent *GW* improves the description of quasiparticle energies^{36–41} as compared to non-self-consistent calculations. Similar conclusions have been obtained for the total energies of atoms,^{37,42,43} molecules,^{44–46} and the homogeneous electron gas.^{27,47,48} For what concerns plasmon satellites in the spectral function, however, Holm and Von Barth have shown that self-consistent *GW* deteriorates the spectral function due to a spurious renormalization of the satellite intensity.⁴⁷ In the following we will limit the discussion to ‘one-shot’ *GW* (or G_0W_0), in which Eq. (6) is evaluated at the first-iteration of the self-consistent procedure. The *GW* self-energy [Eq. (6)] has been obtained from the numerical integration Eq. (89)-(91) of Ref. 9. In Fig. 2 we illustrate the real and imaginary part of the self-energy (in units of the plasmon energy ω_{pl}) for $r_s = 5$. These results, based on the calculation of the RPA dielectric function, are in excellent agreement with the results reported by Lundqvist based on the plasmon-pole approximation.⁶ The *GW* self-energy exhibits a sharp pole at the energy $\epsilon_{\mathbf{k}} \pm \omega_{pl}$, where the $+/-$ signs hold for empty/occupied states. It is evident from Eqs. (6) and (7) that this feature stems primarily from the plasmon peak in the dielectric function, which introduces a singularity in the screened Coulomb interaction W owing to the vanishing ϵ .

Having reviewed the self-energy in the *GW* approximation, we move now to discuss the signatures of plasmon excitations in the spectral function of the HEG. The spectral function is given by:

$$A(\mathbf{k}, \omega) = \frac{1}{\pi} \frac{|\Sigma''_{\mathbf{k}}(\omega)|}{[\omega - \epsilon_{\mathbf{k}} - \Sigma'_{\mathbf{k}}(\omega)]^2 + [\Sigma''_{\mathbf{k}}(\omega)]^2}, \quad (9)$$

where Σ' and Σ'' denote the real and imaginary part of the *GW* self-energy, respectively. In independent-particle

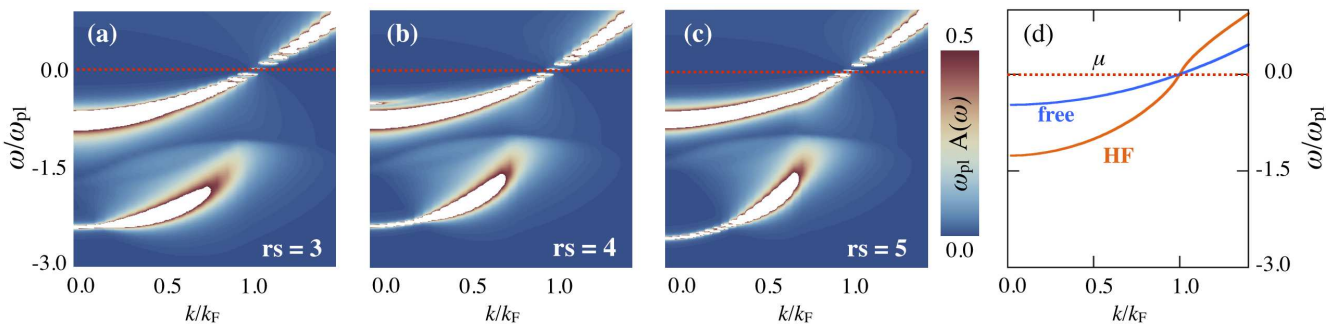


Figure 3. Spectral function of the HEG evaluated in the GW approximation for (a) $r_s = 3$, (b) $r_s = 4$, and (c) $r_s = 5$. Energy and momentum are expressed in units of the plasmon energy ω_{pl} and Fermi momentum k_{F} , respectively. To facilitate a comparison on the same scale, the intensity of the spectral function has been multiplied by ω_{pl} . The red dotted lines indicate the Fermi energy. (d) Quasiparticle energy versus momentum dispersion relations within the Hartree-Fock (HF) approximation, and for non-interacting electrons (free).

approximations, such as the Hartree-Fock approximation or Kohn-Sham density functional theory, the self-energy is static (independent of frequency) and real. The spectral function reduces to a Dirac delta function:

$$A(\mathbf{k}, \omega) = \delta(\omega - \epsilon_{\mathbf{k}} - \Sigma_{\mathbf{k}}). \quad (10)$$

In the case of the Hartree-Fock approximation, the self-energy may be obtained analytically,⁴⁹ and the evaluation of the spectral function is straightforward. The Hartree-Fock spectral function is reported in Fig. 3(d), alongside with the free-electron spectral function. At each \mathbf{k} point, the spectral function of the HEG exhibits Dirac-delta-like structures at the energy of quasiparticle excitations. However, there are no structures that may be attributed to collective excitations induced by electronic correlation. In the GW approximation, on the other hand, the self-energy is characterized by a complex frequency dependence which introduces several additional signatures of electron correlation in the spectral function of the HEG.

The GW spectral function is illustrated in Fig. 3 for the HEG at three different electron densities ($r_s = 3, 4$, and 5). The quasiparticle band is the bright band that appears at $\omega \simeq -\omega_{\text{pl}}$ for $\mathbf{k} = 0$ and increases quadratically with momentum. At variance with the independent particle approximation, the quasiparticle peaks acquire a broadening (vanishing at the Fermi energy) which stems from electronic correlation and is related to the finite lifetime of electronic excitations.

Beside the quadratic quasiparticle band, the spectral function presents pronounced spectral features at energies $1.5\omega_{\text{pl}}$ below the quasiparticle energy. These features are additional solutions of the quasiparticle equation, that is, they arise from the zeros of $\omega - \epsilon_{\mathbf{k}} - \Sigma'_{\mathbf{k}}(\omega)$ in Eq. (9). These spectral features, first reported by Lundqvist, have been originally attributed to plasmarons, a new type of quasiparticle stemming from the strong coupling between holes and plasmons.^{11,12} However, subsequent work have shown that plasmarons are an artifact of the GW approximation.^{8,14} As shown in

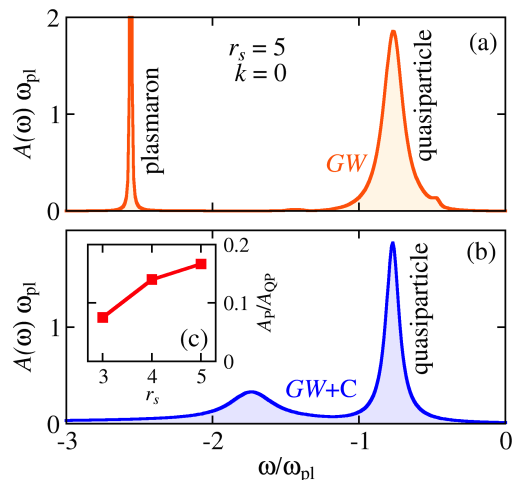


Figure 4. Spectral function of the HEG evaluated from GW (a) and $GW+C$ (b) for $\mathbf{k} = 0$ at $r_s = 5$. (c) Ratio between the intensity of the plasmon satellite and the quasiparticle peak (as obtained from $GW+C$) as a function of r_s .

the following, the cumulant expansion approach provides an ideal way to address this problem, as it improves the plasmon-induced spectral features of the HEG at the same computational cost of a GW calculation.

IV. SPECTRAL FUNCTION FROM THE GW PLUS CUMULANT APPROACH

For the computation of spectral properties, it is common practice to combine the cumulant expansion with the GW approximation. In the resulting $GW+C$ approach, the spectral function can be expressed as:¹⁷

$$A(\mathbf{k}, \omega) = [A^{\text{QP}}(\mathbf{k}, \omega) + A^{\text{QP}}(\mathbf{k}, \omega) * A^{\text{C}}(\mathbf{k}, \omega)]. \quad (11)$$

This expression corresponds to the first-order cumulant expansion, and it ignores processes in which multiple

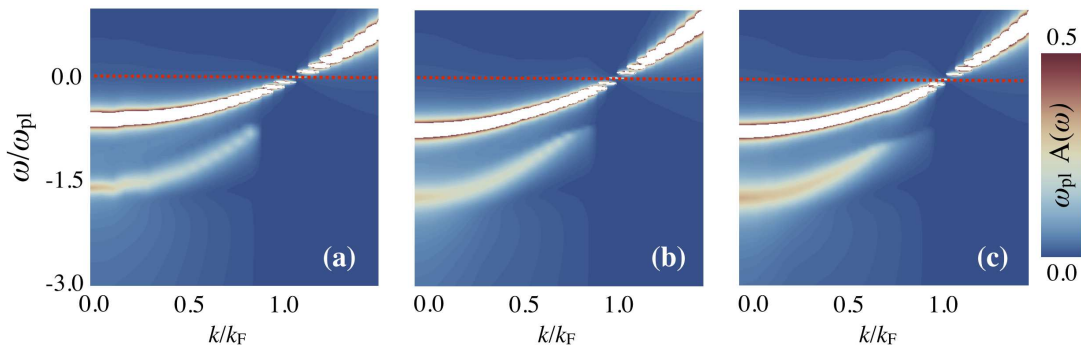


Figure 5. Spectral function of the HEG evaluated from the $GW+C$ approach for (a) $r_s = 3$, (b) $r_s = 4$, and (c) $r_s = 5$. Energy and momentum are expressed in units of the plasmon energy ω_{pl} and Fermi momentum k_{F} , respectively. To facilitate a comparison on the same scale, the spectral function intensity has been multiplied by ω_{pl} . The dashed lines indicate the Fermi energy.

plasmons are excited. Multi-plasmon processes may be accounted for by including higher-order cumulant terms.^{14,20,25} The first term in Eq. (11) is the ordinary quasiparticle spectral function, defined as:

$$A^{\text{QP}}(\mathbf{k}, \omega) = \frac{1}{\pi} \frac{|\Sigma_{\mathbf{k}}''(\epsilon_{\mathbf{k}}^{\text{QP}})|}{[\omega - \epsilon_{\mathbf{k}} - \Sigma_{\mathbf{k}}'(\epsilon_{\mathbf{k}}^{\text{QP}})]^2 + [\Sigma_{\mathbf{k}}''(\epsilon_{\mathbf{k}}^{\text{QP}})]^2}, \quad (12)$$

$\epsilon_{\mathbf{k}}^{\text{QP}} = \epsilon_{\mathbf{k}} + \Sigma_{\mathbf{k}}'(\epsilon_{\mathbf{k}}^{\text{QP}})$ is the quasiparticle energy. The term A^{C} is defined as:

$$A^{\text{C}}(\mathbf{k}, \omega) = \frac{\beta_{\mathbf{k}}(\omega) - \beta_{\mathbf{k}}(\epsilon_{\mathbf{k}}) - (\omega - \epsilon_{\mathbf{k}}) \left. \frac{\partial \beta_{\mathbf{k}}}{\partial \omega} \right|_{\epsilon_{\mathbf{k}}}}{(\omega - \epsilon_{\mathbf{k}})^2}, \quad (13)$$

where $\beta_{\mathbf{k}}(\omega) = \pi^{-1} \text{Im} \Sigma_{\mathbf{k}}(\epsilon_{\mathbf{k}} - \omega) \theta(\mu - \omega)$. Equation (12) accounts for the contribution of quasiparticle excitations to the spectral functions in absence of plasmons. The second term in Eq. (11) accounts for processes in which an electron is emitted and a plasmon is excited.

We evaluated the $GW+C$ angle-resolved spectral function of the HEG by combining the GW self-energy defined in Eq. (6) with the cumulant expansion defined by Eqs. (11)-(13). In Fig. 4 we compare the spectral function at $r_s = 5$ and $\mathbf{k} = 0$ obtained from GW (a) and $GW+C$ (b). The GW and the $GW+C$ approaches provide a similar description of the quasiparticle peak. In the $GW+C$ approach, these features stems from Eq. (12) which coincides with the GW spectral function [Eq. (9)] at the quasiparticle energy $\epsilon_{\mathbf{k}}^{\text{QP}}$. The changes introduced by the cumulant approach affect primarily the low-energy part of the spectral function. At variance with the GW spectral function, whereby the plasmon peak is red-shifted by approximately $1.5\omega_{\text{pl}}$ with respect to the quasiparticle band, the $GW+C$ yields a satellite structure separated by $\sim \omega_{\text{pl}}$ from the quasiparticle energy. As compared to the GW spectral function, these spectral features are more broad and less intense.

Inspecting the angle-resolved spectral function, shown in Fig. 5 for (a) $r_s = 3$, (b) $r_s = 4$, and (c) $r_s = 5$, we note that the dispersion of $GW+C$ satellite follows

closely the momentum dependence of the quasiparticle bands. This indicates that also the HEG is characterized by the formation of a well-defined plasmonic polaron band. Plasmonic polaron bands are a manifestation of the simultaneous excitation of a hole (for instance via the absorption of a photon) and the excitation of a plasmon, and they manifest themselves as broadened band-structure replica, shifted by the plasmon energy with respect to the ordinary quasiparticle bands. These spectral features have recently been predicted in the context of sp -bonded semiconductors^{23,24} and confirmed by angle-resolved photoemission spectroscopy measurements of silicon.³¹ In the case of silicon, plasmonic polaron bands replicate the entire set of valence bands. The HEG, on the other hand, is characterized by a single band. Correspondingly, a single plasmonic polaron band can be observed in Fig. 5.

Our calculations show that the intensity of the satellite features in the $GW+C$ spectral function decreases with increasing density (that is with decreasing r_s), as shown in Fig. 4(c). This behaviour may be attributed to the different scaling of the Coulomb interaction and the kinetic energy with the changes of the electron density:¹ at large densities, the kinetic energy increases more rapidly than the Coulomb interaction and, correspondingly, the effect of electron correlation becomes less important as compared to the kinetic term. In the limit of infinite electron density, the HEG can be approximately described by a non-interacting HEG, as the Coulomb interaction becomes negligible, and the satellite is expected to disappear completely. Conversely, the Coulomb interaction dominates at low densities (large r_s) and one may expect a more pronounced effect of electron correlation on the spectral properties.

V. SUMMARY AND CONCLUSIONS

In summary, we have presented a study of spectral function of the homogeneous electron gas, with an em-

phases on the signatures of electron-plasmon interactions. In particular, we reviewed the analysis of the loss function of the HEG in the random phase approximation and computed the spectral function of the HEG from the GW approximation and the $GW+C$ approach.

At variance with calculations in the independent-particle approximation, the explicit treatment of electron-electron interaction within the GW approximation introduces a non-trivial frequency dependence which, in turn, leads to the emergence of additional low-energy features in the spectral function. At the GW level, for $k < k_F$ the spectral function exhibits the spurious plasmaron peak at an energy of approximately $1.5 \omega_{pl}$ below the quasiparticle energy. A more advanced description of electron-plasmon coupling within the $GW+C$ approach, however, reduces significantly the intensity of the plasmon-induced spectral features and renormalizes their

energy difference to the quasiparticle band to the plasma energy ω_{pl} . Consistently with previous work on semiconductors, the present study reveals that also the HEG is characterized by the emergence of plasmonic polaron bands, that is, plasmon-induced band structure replica red-shifted by the plasmon energy.

ACKNOWLEDGMENTS

This work was supported by the Leverhulme Trust (Grant No. RL-2012-001) and the European Research Council (EU FP7/ERC Grant No. 239578 and EU FP7/Grant No. 604391 Graphene Flagship). Calculations were performed at the Oxford Supercomputing Centre⁵⁰ and at the Oxford Materials Modelling Laboratory.

-
- ¹ P. Nozières and D. Pines, *Theory Of Quantum Liquids*, Advanced Books Classics Series (Westview Press, 1999).
- ² E. Gross, E. Runge, and O. Heinonen, *Many-Particle Theory*, (Taylor & Francis, 1991).
- ³ D. Pines, *Rev. Mod. Phys.* **28**, 184 (1956).
- ⁴ A. W. Blackstock, R. H. Ritchie, and R. D. Birkhoff, *Phys. Rev.* **100**, 1078 (1955).
- ⁵ D. Pines and D. Bohm, *Phys. Rev.* **85**, 338 (1952).
- ⁶ B. Lundqvist, *Physik der kondensierten Materie* **6**, 193 (1967).
- ⁷ L. Hedin and S. Lundqvist (Academic Press, 1970) pp. 1 – 181.
- ⁸ D. C. Langreth, *Phys. Rev. B* **1**, 471 (1970).
- ⁹ L. Hedin, *Phys. Rev.* **139**, A796 (1965).
- ¹⁰ M. S. Hybertsen and S. G. Louie, *Phys. Rev. B* **34**, 5390 (1986).
- ¹¹ B. Lundqvist, *Physik der kondensierten Materie* **6**, 206 (1967).
- ¹² B. Lundqvist, *Physik der kondensierten Materie* **7**, 117 (1968).
- ¹³ A. S. Kheifets, V. A. Sashin, M. Vos, E. Weigold, and F. Aryasetiawan, *Phys. Rev. B* **68**, 233205 (2003).
- ¹⁴ M. Guzzo, G. Lani, F. Sottile, P. Romaniello, M. Gatti, J. J. Kas, J. J. Rehr, M. G. Silly, F. Sirotti, and L. Reining, *Phys. Rev. Lett.* **107**, 166401 (2011).
- ¹⁵ G. Mahan, *Many-Particle Physics* (Springer, 2000).
- ¹⁶ L. Hedin, *Physica Scripta* **21**, 477 (1980).
- ¹⁷ F. Aryasetiawan, L. Hedin, and K. Karlsson, *Phys. Rev. Lett.* **77**, 2268 (1996).
- ¹⁸ L. Hedin, *Journal of Physics: Condensed Matter* **11**, R489 (1999).
- ¹⁹ M. Guzzo, J. J. Kas, L. Sponza, C. Giorgetti, F. Sottile, D. Pierucci, M. G. Silly, F. Sirotti, J. J. Rehr, and L. Reining, *Phys. Rev. B* **89**, 085425 (2014).
- ²⁰ J. S. Zhou, J. J. Kas, L. Sponza, I. Reshetnyak, M. Guzzo, C. Giorgetti, M. Gatti, F. Sottile, J. J. Rehr, and L. Reining, *The Journal of Chemical Physics* **143**, 184109 (2015).
- ²¹ M. Guzzo, J. Kas, F. Sottile, M. Silly, F. Sirotti, J. Rehr, and L. Reining, *The European Physical Journal B* **85**, 324 (2012).
- ²² J. Lischner, D. Vigil-Fowler, and S. G. Louie, *Phys. Rev. Lett.* **110**, 146801 (2013).
- ²³ F. Caruso, H. Lambert, and F. Giustino, *Phys. Rev. Lett.* **114**, 146404 (2015).
- ²⁴ F. Caruso and F. Giustino, *Phys. Rev. B* **92**, 045123 (2015).
- ²⁵ J. J. Kas, J. J. Rehr, and L. Reining, *Phys. Rev. B* **90**, 085112 (2014).
- ²⁶ J. Lischner, D. Vigil-Fowler, and S. G. Louie, *Phys. Rev. B* **89**, 125430 (2014).
- ²⁷ B. Holm and F. Aryasetiawan, *Phys. Rev. B* **62**, 4858 (2000).
- ²⁸ B. Gumhalter, *Phys. Rev. B* **72**, 165406 (2005).
- ²⁹ B. Gumhalter, *Progress in Surface Science* **87**, 163 (2012).
- ³⁰ V. M. Silkin, P. Lazić, N. Došlić, H. Petek, and B. Gumhalter, *Phys. Rev. B* **92**, 155405 (2015).
- ³¹ J. Lischner, G. K. Pálsson, D. Vigil-Fowler, S. Nemsak, J. Avila, M. C. Asensio, C. S. Fadley, and S. G. Louie, *Phys. Rev. B* **91**, 205113 (2015).
- ³² P. Nozières and D. Pines, *Phys. Rev.* **113**, 1254 (1959).
- ³³ A. L. Fetter and J. D. Walecka, *Quantum Theory of Many-Particle Systems* (Dover Publications, 2003).
- ³⁴ For $\mathbf{q} = 0$ this condition yields the plasma frequency $\omega_{pl} = \omega_{pl}(\mathbf{q} = 0) = \sqrt{4\pi n e^2 / m}$, n being the HEG density.
- ³⁵ D. Pines, *Elementary Excitations in Solids: Lectures on Protons, Electrons and Phonons*, Advanced book classics (Advanced Book Program, Perseus Books, 1999).
- ³⁶ A. Stan, N. E. Dahlen, and R. van Leeuwen, *EPL (Europhysics Letters)* **76**, 298 (2006).
- ³⁷ A. Stan, N. E. Dahlen, and R. van Leeuwen, *J. Chem. Phys.* **130**, 114105 (2009).
- ³⁸ C. Rostgaard, K. W. Jacobsen, and K. S. Thygesen, *Phys. Rev. B* **81**, 085103 (2010).
- ³⁹ N. Marom, F. Caruso, X. Ren, O. T. Hofmann, T. Körzdörfer, J. R. Chelikowsky, A. Rubio, M. Scheffler, and P. Rinke, *Phys. Rev. B* **86**, 245127 (2012).
- ⁴⁰ F. Caruso, P. Rinke, X. Ren, A. Rubio, and M. Scheffler, *Phys. Rev. B* **88**, 075105 (2013).
- ⁴¹ P. Koval, D. Foerster, and D. Sánchez-Portal, *Phys. Rev. B* **89**, 155417 (2014).
- ⁴² N. E. Dahlen and R. van Leeuwen, *J. Chem. Phys.* **122**, 164102 (2005).
- ⁴³ N. E. Dahlen, R. van Leeuwen, and U. von Barth, *Phys. Rev. A* **73**, 012511 (2006).

- ⁴⁴ F. Caruso, P. Rinke, X. Ren, M. Scheffler, and A. Rubio, *Phys. Rev. B* **86**, 081102 (2012).
- ⁴⁵ F. Caruso, D. R. Rohr, M. Hellgren, X. Ren, P. Rinke, A. Rubio, and M. Scheffler, *Phys. Rev. Lett.* **110**, 146403 (2013).
- ⁴⁶ M. Hellgren, F. Caruso, D. R. Rohr, X. Ren, A. Rubio, M. Scheffler, and P. Rinke, *Phys. Rev. B* **91**, 165110 (2015).
- ⁴⁷ B. Holm and U. von Barth, *Phys. Rev. B* **57**, 2108 (1998).
- ⁴⁸ B. Holm, *Phys. Rev. Lett.* **83**, 788 (1999).
- ⁴⁹ R. Martin, *Electronic Structure: Basic Theory and Practical Methods* (Cambridge University Press, 2004).
- ⁵⁰ A. Richards, *University of Oxford Advanced Research Computing* (2015).